Supplementary Information

Assembled Collagen Films Modified by Polyacrylic Acid with Improved Mechanical Properties via Mineralization

Xiaohui Chen, [a b] Zhilin Huang, [a b] Shuyun Zhang, [* c] Hong Li, [* a b]

[a] College of Chemistry and Materials Science, Jinan University, Guangdong, 511443, P.R. China.

[b] Engineering Research Center of Artificial Organs and Materials, Jinan University, Guangdong, 510632, P.R. China.

[c] Guangdong Second Provincial General Hospital, Postdoctoral Research Station of Basic Medicine, School of Medicine, Jinan University, Guangdong, 510220, P.R. China.

* Corresponding authors:

These two authors worked on this study as co-corresponding authors.

Research Assistant Shuyun Zhang, Ph. D

Guangdong Second Provincial General Hospital, Postdoctoral Research Station of Basic Medicine, School of Medicine, Jinan University, Guangdong, 510220, P.R. China.

E-mail: shuyunzhang@jnu.edu.cn

Tel.: +86-20-37331541

Professor Hong Li, Ph. D

College of Chemistry and Materials Science, Jinan University, No. 855, Eest Xingye Avenue, Guangzhou, Guangdong, 510632, People's Republic of China.

E-mail: tlihong@jnu.edu.cn

Tel.: +86-20-37331541

S1. Methods

S1.1. Preparation of 1.5-fold simulated body fluids (1.5× SBF)

Add 600 mL deionized water to a plastic beaker (2 L) and place it in a constant temperature water bath at 37 ^{o}C. When the temperature of the water in the beaker reaches 37 ^{o}C, NaCl, $NaHCO_3$, KCl, K_2HPO_4, $MgCl_2$, HCl, $CaCl_2$ and Na_2SO_4 are added in sequence. It was necessary to add the latter reagent after the former reagent is completely dissolved. Finally, the pH was adjusted to 7.4 with trishydroxymethylaminomethane (Tris) and HCl. After the solution was cooled to room temperature, the volume was fixed with a volumetric bottle to 1 L, so that the final concentration of each ion in the solution is shown in Table S1 below.

Table 1. The concentration of each ion in 1.5-fold simulated body fluids

ion	Concentration (mmol/L)
Na^{+}	142
K^{+}	5
Mg^{2+}	1.5
Ca^{2+}	3.75
Cl^{-}	148.8
HCO^{3-}	4.2
HPO_4^{2-}	1.5
SO_4^{2-}	0.5

S1.2. Characterization of PAA-Collagen

Collagen was dissolved in 1% acetic acid solution and thoroughly mixed to obtain 0.5 mg/mL collagen solution. The other operations in the control group were the same as those in the experimental group except that PAA was not added. In the experimental group, 10 mg PAA was added to 2 mL MES buffer (pH =5.5), 1.235 mg EDC and 1.5 mg NHS were added for 15 minutes, then 5 mL PBS buffer (pH =7.5) was added, and finally 3 mL of the above collagen solution was added. After reaction for 2 hours, it was added into the quartz UV cuvette and placed in the UV spectrophotometer (UV-Vis, TU-1810, Beijing Purkinje, China), with a scanning wavelength range of 200 nm to 350 nm.

The TNBS (trinitrobenzenesulfonic acid) assay[1] was used to determine the crosslinking degree of PAA: 10 ± 1 mg of Bare-collagen and PAA-collagen were added to the glass bottle containing 1 mL of 4% $NaHCO_3$ solution, and incubated at room temperature for 2 hours. 1 mL of 0.1% TNBS solution (dissolved in 4% $NaHCO_3$) was added to various liquids, and kept at a constant temperature in a 40 °C water bath in the dark for 2 hours. Then add 3 mL of 6 M HCl solution and incubate the mixture in a 60 °C water bath for 1.5 hours. After 3 minutes of ultrasound, continue to incubate for 1 hour. After cooling the mixture to room temperature, dilute it to 10 mL and take 1.5 mL of each diluted solution. Test the absorbance of the above samples using UV spectrophotometer, with a scanning measurement wavelength range of 345 nm. 5 parallel samples per group. The cross linking degree (CD) was determined according to the following equation:

$$CD = 1 - \left\{ \frac{\left(\frac{absorption1}{m1} \right)}{\left(\frac{absorption0}{m0} \right)} \right\} \times 100\% \#(1)$$

Among them, m_1 is the mass of PAA-collagen, m_0 is the mass of Bare-collagen.

S1.3. Swelling Ratio and Total Surface Area

The rectangular sample with 5 × 1 × 0.02 cm were weighed and the initial mass was recorded as W_0. Then, the films were immersed in deionized water at 37 °C and removed after 2, 10, 20, 30, 60, and 120 minutes. The films were reweighed and their mass was recorded as W_1. The swelling ratio was determined according to the following equation:[2]

$$Swelling\ ratio(\%) = \frac{W1\ -\ W0}{W0} \times 100\% \#(2)$$

The length and width of the film are measured, the thickness of the film before and after swelling is recorded, and the total surface area is calculated from the rectangular shape and size.

S2. Results and discussion

S2.1. Properties of Self-extracted Oriented Collagen Film

The secondary structure of the self-extracted collagen was analyzed by infrared spectroscopy, ultraviolet spectrophotometer and circular dichroism. Infrared spectra (Fig. 1B) and circular dichroism (Fig. 1D) are presented in the text. Under ultraviolet light, type I collagen had a steeper absorption peak at about 226 nm, whereas the PAA-collagen absorption peak shifted to 235 nm (Fig. S1). To summarize, self-extracted collagen has triple-helical structure and the structure of collagen was not destroyed by modification.

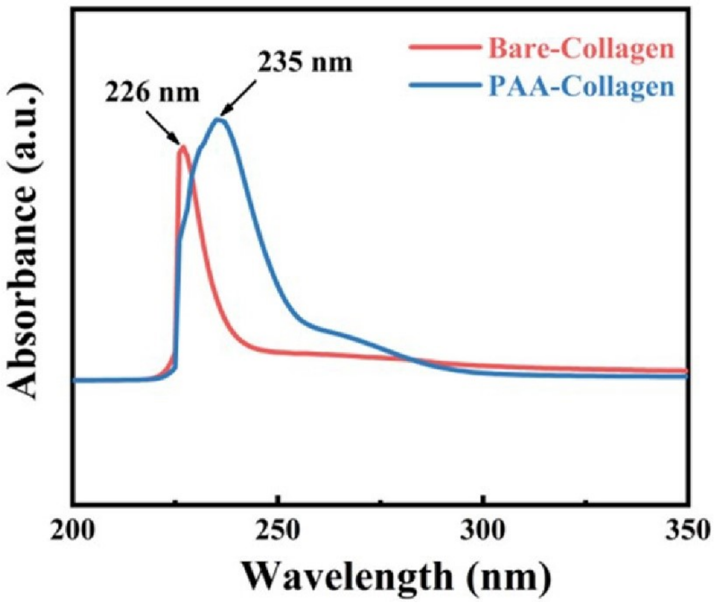

Fig. S1. UV-Vis spectra of Bare-collagen and PAA-collagen solutions.

S2.2. Characterization of PAA-collagen Film

Degrees of cross-linking (%) of PAA can be calculated to be 13.59 ± 0.70%.

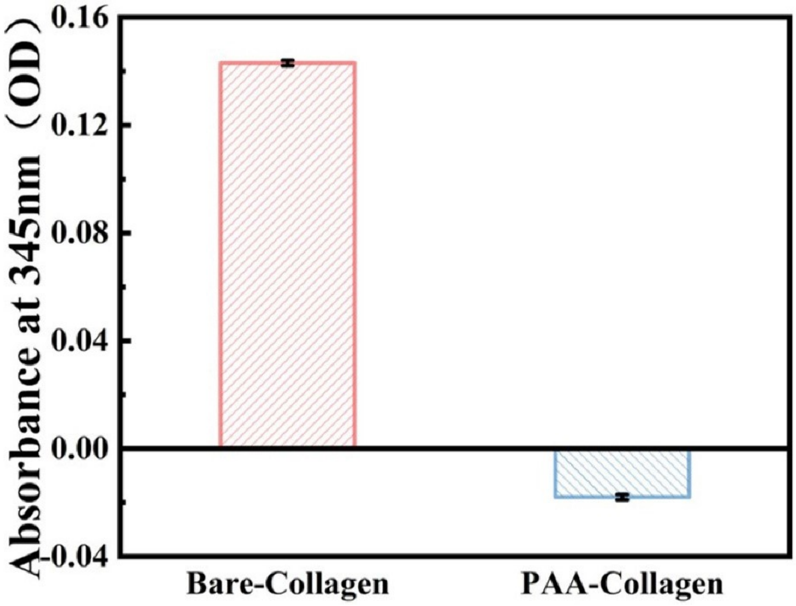

Fig. S2. The absorbance image of TNBS assay of Bare-collagen and PAA-collagen film.

S2.3. Mineralization of Collagen Materials

On the surface of COL + SBF sample (Fig. S3A), the growth of mineral crystals is very concentrated and only exists in a small area of the collagen membrane. This is because in the absence of additives, CaP settles on the fibrils' surface mainly in the form of random, large deposits, which keep accord with the previous report.[3] The morphology of mineralized spheres on COL + CPAM-SBF (Fig. S3B) was similar to that on PAA-COL + SBF (Fig. S3C), but the stacking of HAP crystals is relatively less. In the two groups, PAA grafted on collagen surface and CPAM in the mineralized solution mainly played a role in stabilizing ACP, respectively, so HAP dispersed and deposited on collagen surface.[4] Compare to the loose-stacked mineral particles of the other samples, the HAP crystals on the PAA-COL + CPAM-SBF film (Fig. S3D) are completely covered the surface with a certain thickness to form a continuous and uniform coating. The carboxyl group on PAA molecule has a strong coordination ability with metal ions, while CPAM inhibits the aggregation of ACP, making part of ACP enter the collagen fiber under the action of capillary force. The ionic bonding force between calcium and phosphate ions is greater than that between PAA-Ca^{2+} and CPAM-phosphate ions, respectively, resulting in the formation of a dense HAP coating on the surface, as well the remarkable extrafibrillar mineralization.[5] That implied PAA-COL + CPAM-SBF accelerated the crystal nucleation and growth most efficiently. EDS (Fig. S3E-H) shows that the crystals are mainly composed of Ca and P elements. By calculating the calcium-phosphorus ratio, it is found that after 5 days, the Ca/P ratio in the COL+SBF, COL+CPAM-SBF, PAA-COL + SBF and PAA-COL + CPAM-SBF group was about 1.36, 1.41, 1.53 and 1.59, respectively.

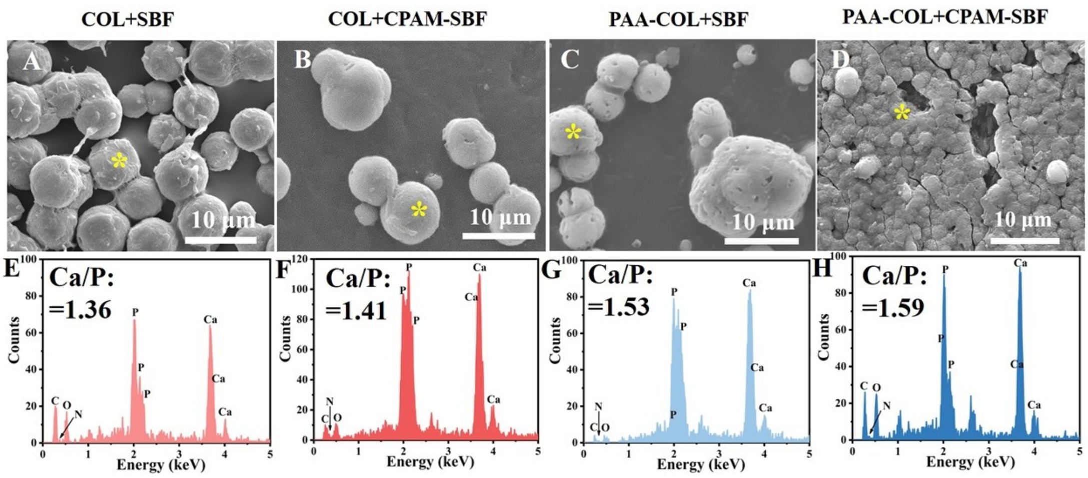

Fig. S3. (A-D) Magnified images of the sequential marked areas in Fig. 3(D-G), respectively. (E-H) The respective EDS traces of the yellow asterisks in (A-D), respectively.

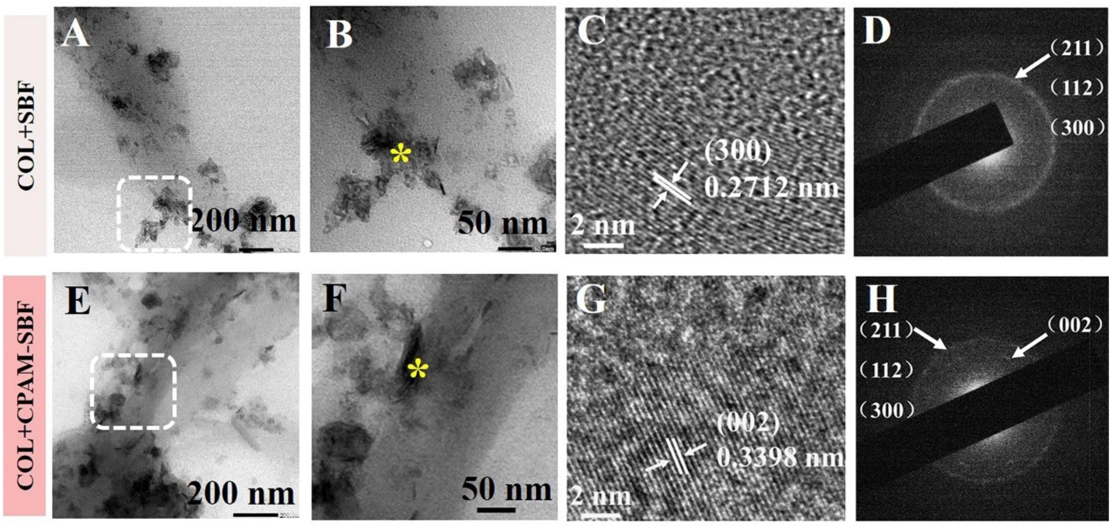

Fig. S4. (A) TEM image of COL + SBF after 5 days of mineralization. (B) HRTEM image of the sequential marked areas in (A). (C) HRTEM image of the yellow asterisks in (B). (D) SAED image of the yellow asterisks in (B). (E) TEM image of COL + CPAM-SBF after 5 days of mineralization. (F) HRTEM image of the sequential marked areas in (E). (G) HRTEM image of the yellow asterisks in (F). (H) SAED image of the yellow asterisks in (F).

S2.4. Mechanical Properties of Mineralized Collagen Films in Wet State

Compared with the mechanical properties of collagen in a dry state, the mechanical properties of samples have decreased in the wet state, but it can still be clearly observed that the tensile strength (Fig. S5B), elastic modulus (Fig. S5C) of PAA-COL + SBF and PAA-COL + CPAM-SBF were greater than those of other groups under the same conditions. PAA-COL + CPAM-SBF can effectively enhance the wet mechanical properties of mineralized collagen films.

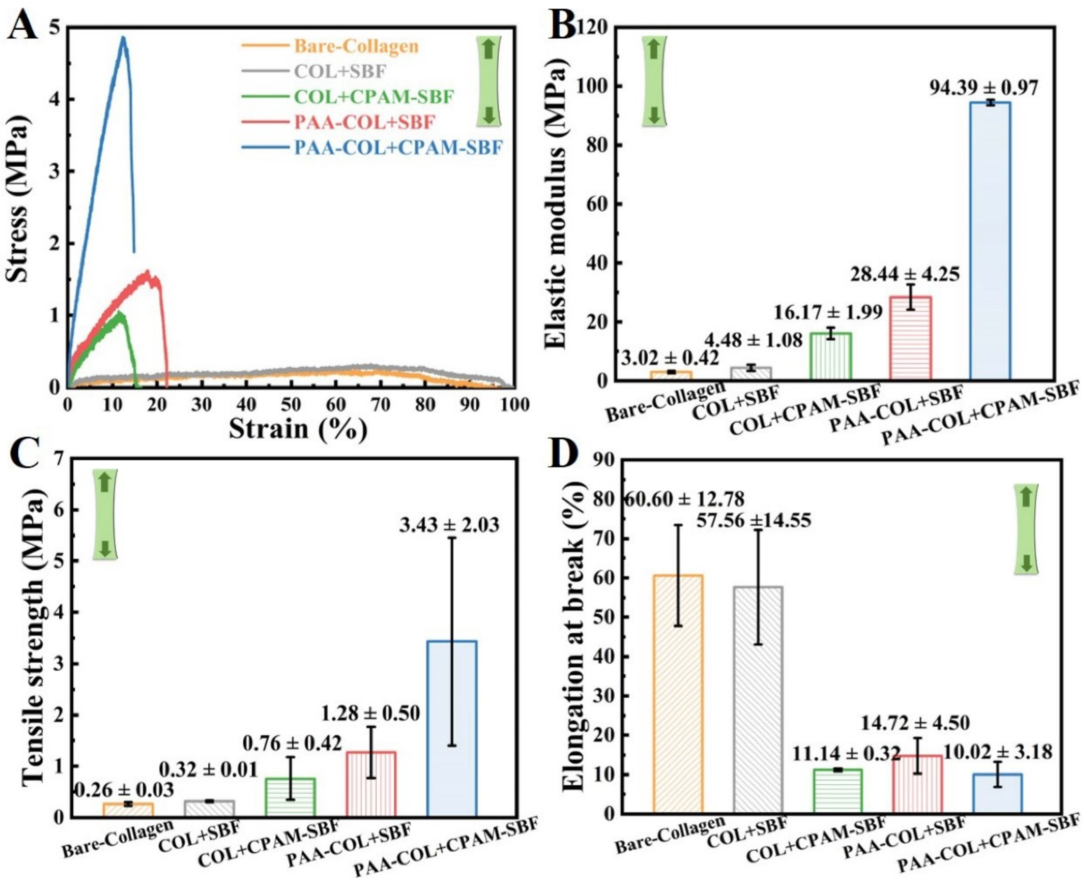

Fig. S5. Mechanical properties of films under wet condition: (A) Stress-strain curve. (B) Elastic modulus. (C) Tensile strength. (D) Elongation at break.

S2.5. Swelling Ratio and Total Surface Area of Mineralized Collagen Films

Fig. S6 shows the swelling ratio and total surface area of the collagen material. It can be found that after immersing the different collagen films in water for 60 minutes, the swelling balance of all groups was reached. In addition, all films expanded to more than 100%, which may be due to the swelling of the polymer chain segments of the collagen itself, and the water absorption of the tiny fiber gaps, thus increasing the total surface area of the sample. Among them, the swelling ratio of PAA-COL + SBF and PAA-COL + CPAM-SBF was lower, which may be due to the cross-linking of the collagen fiber network modified by PAA, which limited the swelling of their collagen films. In addition, the mineral crystals within the collagen membrane also hinder the swelling of the collagen fiber network.[6]

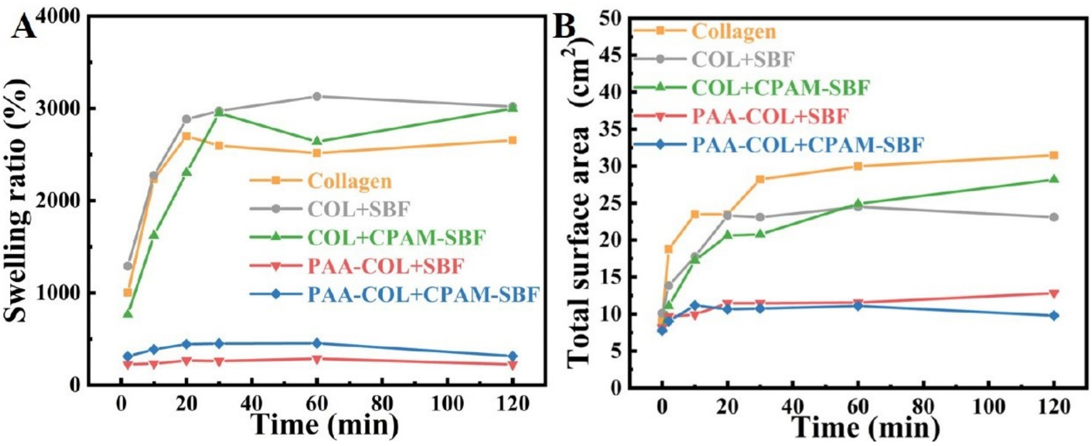

Fig. S6. (A) Swelling ratio, (B) Total surface area of the non-mineralized and mineralized collagen films.

S2.6. The Mineralization Mechanism of Assembled Collagen Films

First, the negatively charged carboxyl group of PAA can have a short-range electrostatic interaction with Ca^{2+} and then accelerate the conversion of ACP to HAP.[7,8] In the pH variation diagram of SBF (Fig. S7B), the rapid decrease of pH at the beginning can be attributed to the formation of ACP, then ACP induces HAP nucleation and the pH remains relatively stable.[9,10] The ion consumption during mineralization leads to a decrease in the concentration of calcium and phosphate ions, so the pH rises somewhat. After 24 hours, the pH of the two groups of PAA-modified collagen decreased less than that of the unmodified collagen group, indicating that PAA provided additional nucleation sites for HAP nucleation on collagen. Fig. S7C showed that the induction time of PAA modified group is shorter, that is, PAA can accelerate the conversion of ACP into HAP.

Previous studies have shown that the smaller the ACP particle size, the easier it is to enter collagen fibers.[4] NCPs are known to affect the stability and particle size distribution of ACP.[11] Secondly, CPAM is added to 1.5× SBF solution. The effect of CPAM on the morphology of ACP can be observed by TEM. Among them, Fig. S7D is the TEM image of SBF in the control group, and Image J shown that the diameter of its spherical ACP is 48.3 ± 8.83 nm. Fig. S7G shows the TEM image of CPAM-SBF, which shows the ACP diameter is 13.9 ± 2.79 nm. This indicated that the ACP size was decreased after 1 day of adding CPAM. Fig. S7E and Fig. S7H illustrated ACP adhesion to collagen fibril on the first day. Fig. S7F and Fig. S7I showed the changes in nanoparticle size between the first day of fresh preparation of SBF and CPAM-SBF and the fifth day of placement without adding collagen membrane mineralization. In Fig. 7G, the ACP on the first day was 48.05 nm and 372.04 nm, and the particle size increases to 73.69 nm and 402.9 nm and 4594 nm after 5 days of placement. However, in Fig. 7J, there is a peak of 4000 nm in the CPAM-SBF on the first and fifth day, and the intensity of this size is unchanged, indicating that this is CPAM formed after aggregation. The CPAM-ACP on the first day are 0.68 nm and 157.4 nm, and the particle size increases to 63.43 nm and 556.8 nm after 5 days of placement. In summary, CPAM as a polycationic electrolyte, can coordinate with hydrogen phosphate and weaken the binding of hydrogen phosphate to Ca^{2+} to inhibit ACP aggregation.[5,8,12] The stress assembled collagen membrane before mineralization is used to simulate the self-assembled collagen fibers in *vivo* and drive ACP precursors to be immersed into collagen fibers.[13] In addition, the high molecular weight of CPAM results in high osmotic pressure, and the stabilized ACP with small particle size can penetrate into the collagen fiber through capillary penetration force.[14]

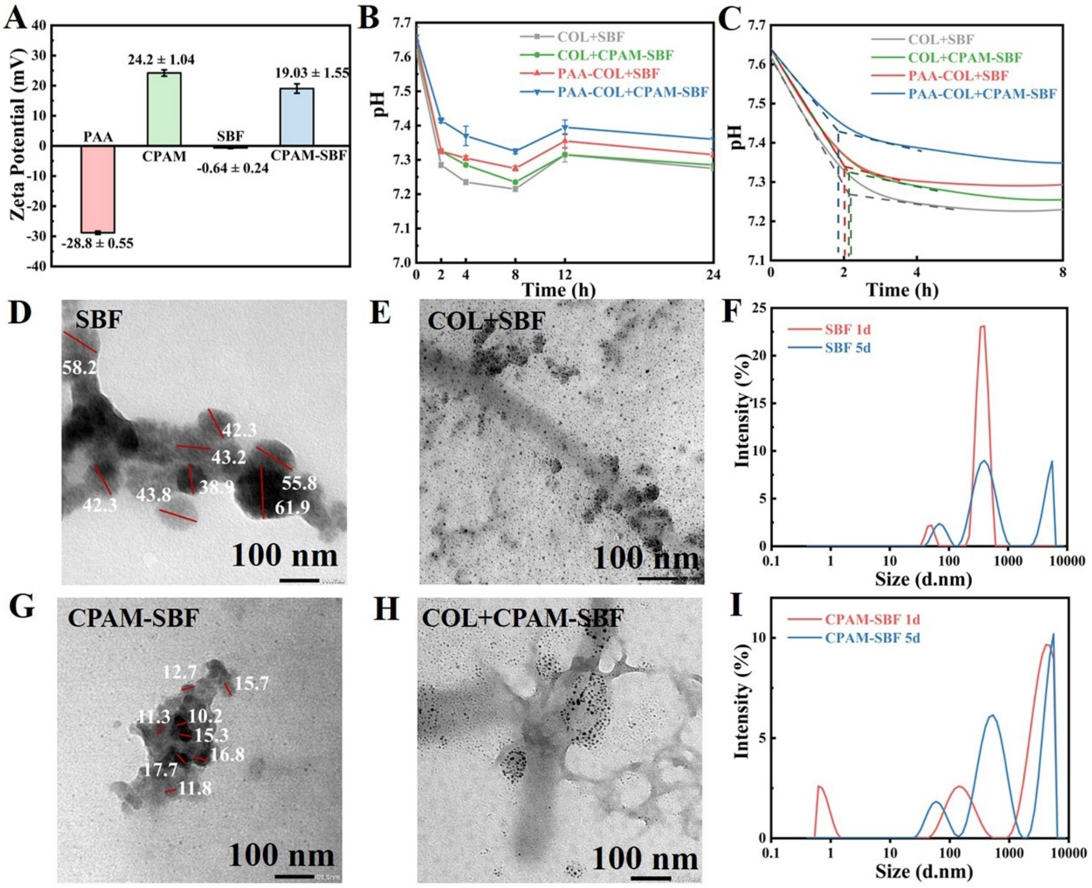

Fig. S7. (A) Zeta potential diagram of the PAA, CPAM, SBF, CPAM-SBF solution. (B) The pH curves of COL+SBF, COL+CPAM-SBF, PAA-COL + SBF and PAA-COL + CPAM-SBF in the same mineralized condition. (C) The pH induction curve within 8 hours of mineralization. (D) and (E) are the TEM images of amorphous calcium phosphate in SBF and CPAM-SBF on the first day, respectively. (F) and (G) are TEM images of amorphous calcium phosphate in COL + SBF group and COL + CPAM-SBF group on the first day, respectively. (H) and (I) are the Nano size changes of mineralized liquid SBF and CPAM-SBF on the first day of fresh preparation and on the fifth day of placement.

S3. In *vitro* Cell Biocompatibility

Bone repair materials need to have good biocompatibility. The cell proliferation was evaluated by CCK-8, and the proliferation level of PAA modified collagen was not significantly changed. PAA-COL + CPAM-SBF has good biocompatibility and can be used as bone repair material.

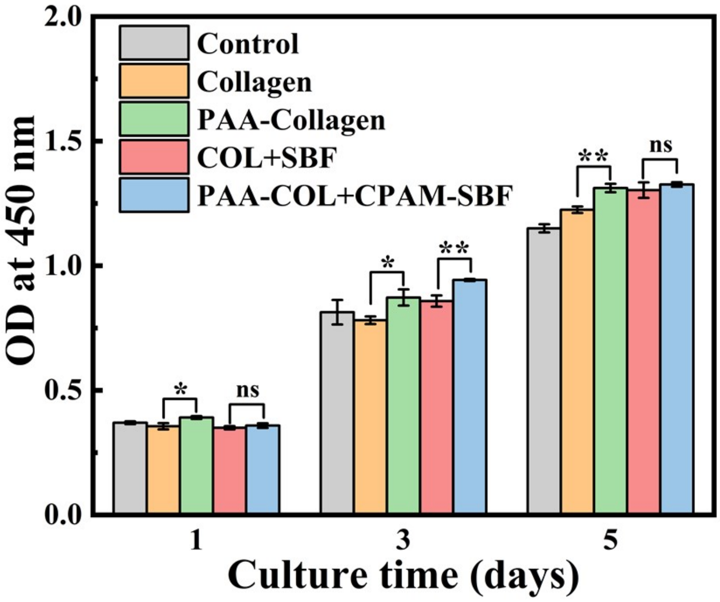

Fig. S8. The proliferation of MC3T3-E1 cells cultured on the membranes for 1, 3, and 5 days, evaluated by CCK-8 assay.

References

1. N. Nagai, S. Yunoki, T. Suzuki, M. Sakata, K. Tajima and M. Munekata, *J. Biosci. Bioeng.*, 2004, **97**, 389-394.
2. C. Liu, L. Jiang, W. Du, X. Cheng, Z. Zhao, J. Wang and X. Jian, *J. Appl. Polym. Sci.*, 2023, **140**, e54275.
3. L. B. Gower, *Chem. Rev.*, 2008, **108**, 4551-4627.
4. F. Nudelman, K. Pieterse, A. George, P. H. Bomans, H. Friedrich, L. J. Brylka, P. A. Hilbers, G. de With and N. A. Sommerdijk, *Nat. Mater.*, 2010, **9**, 1004-1009.
5. T. Du, Z. Li, X. Li, X. Niu and Y. Fan, *Mater. Today Commun.*, 2022, **30**, 103064.
6. F. Liu, K. Zhu, Y. Ma, Z. Yu, B.-S. Chiou, M. Jia, M. Chen and F. Zhong, *Food Hydrocolloids*, 2023, **139**, 108579.

7. L. B. Gower and D. J. Odom, *J. Cryst. Growth*, 2000, **210**, 719-734.
8. Q. Song, K. Jiao, L. Tonggu, L. Wang, S. Zhang, Y. Yang, L. Zhang, J. Bian, D. Hao and C. Wang, *Sci. Adv.*, 2019, **5**, eaav9075.
9. S. Jiang, Y. Chen, H. Pan, Y.-J. Zhang and R. Tang, *Phys. Chem. Chem. Phys.* 2013, **15**, 12530-12533.
10. H. Wu, C. Shao, J. Shi, Z. Hu, Y. Zhou, Z. Chen, R. Tang, Z. Xie and W. Jin, *Carbohydr. Polym.*, 2023, **319**, 121174.
11. A. Indurkar, R. Choudhary, K. Rubenis and J. Locs, *Front. Bioeng. Biotechnol.*, 2023, **11**, 1150037.
12. L.-N. Niu, S. E. Jee, K. Jiao, L. Tonggu, M. Li, L. Wang, Y.-D. Yang, J.-H. Bian, L. Breschi and S. S. Jang, *Nature materials*, 2017, **16**, 370-378.
13. M. Lin, H. Liu, J. Deng, R. An, M. Shen, Y. Li and X. Zhang, *J. Mater. Sci. Technol.*, 2019, **35**, 1894-1905.
14. M. J. Olszta, X. Cheng, S. S. Jee, R. Kumar, Y.-Y. Kim, M. J. Kaufman, E. P. Douglas and L. B. Gower, *Mater. Sci. Eng. R Rep.*, 2007, **58**, 77-116.